

PAPER • OPEN ACCESS

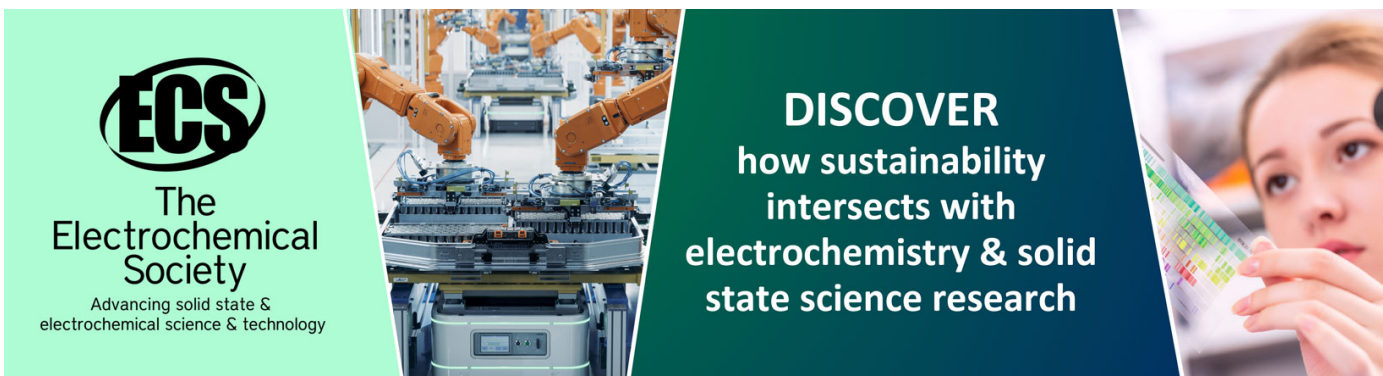
Stability investigation of a high number density Pt₁/Fe₂O₃ single-atom catalyst under different gas environments by HAADF-STEM

To cite this article: Sabin Duan *et al* 2018 *Nanotechnology* **29** 204002

View the [article online](#) for updates and enhancements.

You may also like

- [Review—Non-Noble Metal-Based Single-Atom Catalysts for Efficient Electrochemical CO₂ Reduction Reaction](#)
Hyeonuk Choi, Dong-Kyu Lee, Mi-Kyung Han et al.
- [Single-atom catalyst cathodes for lithium–oxygen batteries: a review](#)
Xin Lei, Bo Liu, Payam Ahmadian Koudakan et al.
- [Ultrafast synthetic strategies under extreme heating conditions toward single-atom catalysts](#)
Guanchao He, Minmin Yan, Haisheng Gong et al.



ECS
The
Electrochemical
Society
Advancing solid state &
electrochemical science & technology

DISCOVER
how sustainability
intersects with
electrochemistry & solid
state science research

Stability investigation of a high number density Pt₁/Fe₂O₃ single-atom catalyst under different gas environments by HAADF-STEM

Sibin Duan^{1,2} , Rongming Wang^{1,3}  and Jingyue Liu^{2,3}

¹ Beijing Key Laboratory for Magneto-Photoelectrical Composite and Interface Science, School of Mathematics and Physics, University of Science and Technology Beijing, Beijing 100083, People's Republic of China

² Department of Physics, Arizona State University, Tempe, Arizona 85287, United States of America

E-mail: rmwang@ustb.edu.cn and Jingyue.Liu@asu.edu

Received 29 December 2017, revised 12 February 2018

Accepted for publication 23 February 2018

Published 22 March 2018



Abstract

Catalysis by supported single metal atoms has demonstrated tremendous potential for practical applications due to their unique catalytic properties. Unless they are strongly anchored to the support surfaces, supported single atoms, however, are thermodynamically unstable, which poses a major obstacle for broad applications of single-atom catalysts (SACs). In order to develop strategies to improve the stability of SACs, we need to understand the intrinsic nature of the sintering processes of supported single metal atoms, especially under various gas environments that are relevant to important catalytic reactions. We report on the synthesis of high number density Pt₁/Fe₂O₃ SACs using a facial strong adsorption method and the study of the mobility of these supported Pt single atoms at 250 °C under various gas environments that are relevant to CO oxidation, water–gas shift, and hydrogenation reactions. Under the oxidative gas environment, Fe₂O₃ supported Pt single atoms are stable even at high temperatures. The presence of either CO or H₂ molecules in the gas environment, however, facilitates the movement of the Pt atoms. The strong interaction between CO and Pt weakens the binding between the Pt atoms and the support, facilitating the movement of the Pt single atoms. The dissociation of H₂ molecules on the Pt atoms and their subsequent interaction with the oxygen species of the support surfaces dislodge the surface oxygen anchored Pt atoms, resulting in the formation of Pt clusters. The addition of H₂O molecules to the CO or H₂ significantly accelerates the sintering of the Fe₂O₃ supported Pt single atoms. An anchoring-site determined sintering mechanism is further proposed, which is related to the metal–support interaction.

Supplementary material for this article is available [online](#)

Keywords: single-atom catalyst, metal–support interaction, sintering, catalyst stability, heterogeneous catalysis

(Some figures may appear in colour only in the online journal)

³ Authors to whom any correspondence should be addressed.



Original content from this work may be used under the terms of the [Creative Commons Attribution 3.0 licence](#). Any further distribution of this work must maintain attribution to the author(s) and the title of the work, journal citation and DOI.

1. Introduction

Supported metal catalysts are widely used for both fundamental research and industrial applications because of their excellent activity, selectivity, and stability [1–3]. Supported Pt catalysts are extensively applied in many important chemical reactions including emission control of toxic gases,

producing of chemicals, and energy conversion in fuel cells [4–6]. Both theoretical modeling and experimental research on the catalytic properties of Pt based catalysts have been extensively studied [7–10].

Metal–support interaction plays an important role in determining the catalytic performance of supported metal catalysts [11, 12]. The nature of the metal–support interaction depends on many parameters including particle size, quality of the interfaces, the surface structure and chemistry of the support materials [13–16]. Among them, the metal nanoparticle size has proven to be crucial in modulating the metal–support interaction. Many research studies have reported that the catalytic activities can be well regulated by controlling the metal particle size [15, 17, 18]. For example, in the Pt/Fe₂O₃ system, the particle size of Pt colloid influenced the chemical states of Pt species and the strength of the metal–support interactions, and it is suggested that suitable metal–support interactions played a crucial role in determining the redox properties of the catalysts, thus being beneficial to the oxidation of CO at low temperature [19]. Additionally, for hydrotalcite supported Pt nanoparticles, the activity of propane conversion in the propane dehydrogenation process increases with the reduction of Pt nanoparticle size, while the selectivity to propylene performs in an inverse way [20]. Accordingly, downsizing the metal particle size in the supported metal catalysts has been one of the most important targets in the catalysis research field [21, 22]. Single-atom catalysts (SACs), which reach the size limitation of supported metal catalysts and maximize the efficiency of the active metals, have been of increased interest for both fundamental study and industrial applications during the past few years [23–25]. As a pioneering work, a Pt₁/FeO_x SAC was practically fabricated by a coprecipitation method and exhibits very high activity and stability for both CO oxidation and preferential oxidation of CO in H₂, attributed to the partially vacant 5*d* orbitals of positively charged, high-valent Pt atoms [24]. Much literatures has confirmed the outstanding performance of SACs compared to their nanoparticle or cluster counterparts. And it has also been verified that in some supported metal catalysts that consist of clusters or nanoparticles, the atomically dispersed metal atoms are the most important active sites during the catalytic reactions [23, 26, 27]. Many works have been devoted to the synthesis of SACs, among which the adsorption approach has proven to be an efficient way to anchor metal atoms onto the surface of the as-prepared supports, taking advantage of the metal–support interactions [28–30].

For supported metal catalysts, stability is another important factor that restricts their industrial application. Sintering of metal components during the heating process or catalytic reactions often leads a loss of activity or selectivity [31, 32]. The sintering of supported metal catalysts has been intensively studied in recent years, and the strong metal–support interaction has proven to be vital for the stability of heterogeneous catalysts [25, 33–35]. As for the SACs, due to the high surface-free energy and the low coordination number of metal single atoms, supported metal atoms are thermodynamically unstable and easy to sinter during catalytic

reactions, especially at high reaction temperatures [36–39]. The investigation of the stability of supported single metal atoms under a specific gas environment can help us understand the sintering mechanisms of SACs during catalytic reactions and thus provide insights into developing stable SACs for practical applications. Researchers have used scanning tunneling microscopy to follow the evolution of supported Pt and Pd atoms in model catalysts under various environments illustrating the role of gas molecules in the anchoring and sintering of metal atoms [40–42]. However only a few reports have been published on this subject [41–43], and these are still somewhat limited, especially for the stability of SACs with a high number density studied by aberration-corrected (AC) electron microscopy, which is a convincing and intuitive approach to directly image the single metal atoms, clusters, and nanoparticles in the supported metal catalysts.

Here, a Pt₁/Fe₂O₃ SAC with a Pt₁ number density as high as 1.2 atom nm^{−2} was synthesized by a facial wet chemical method. We further investigated the mobility of high number density Pt single atoms in a Pt₁/Fe₂O₃ SAC at a moderate temperature under various gas environments that are relevant for CO oxidation, water–gas shift, and hydrogenation reactions.

2. Method

2.1. Catalysts preparation

2.1.1. Chemicals and materials. Ferric nitrate (Fe(NO₃)₃ · 9H₂O, Baker Analyzed, ACS reagent), chloroplatinic acid hexahydrate (H₂PtCl₆ · 6H₂O, Sigma-Aldrich, ACS reagent, ≥37.50% Pt basis), and sodium carbonate (Na₂CO₃, Sigma-Aldrich, ≥99.5%) were used as received without any further purification. Deionized water was purified in a Barnstead NANOpure II system with a resistivity better than 17.5 MΩ cm.

2.1.2. Synthesis of the Fe₂O₃. The Fe₂O₃ support was synthesized by a precipitation method with Fe(NO₃)₃ · 9H₂O as the precursor and Na₂CO₃ as the precipitant. In a typical synthesis procedure, an Fe(NO₃)₃ · 9H₂O aqueous solution (40 ml, 1.0 M) was added dropwise into the Na₂CO₃ aqueous solution (150 ml, 0.7 M) at 50 °C with vigorous stirring. The precipitate was filtered, washed, dried, and calcined at 400 °C for 5 h.

2.1.3. Synthesis of the Pt₁/Fe₂O₃. A Pt SAC with a high number density was synthesized by a modified adsorption method based on our previous research. In a typical synthesis, the prepared Fe₂O₃ (1.0 g) was dissolved in 150 ml of deionized water. A H₂PtCl₆ aqueous solution (100 ml, 0.615 mM) was added dropwise into the Fe₂O₃ suspension under stirring at room temperature. After aging for 4 h, the precipitate was filtered, washed, dried at 60 °C for 5 h, and calcined at 300 °C for 4 h in air, and is denoted as Pt₁/Fe₂O₃. The accurate Pt loadings in the catalysts were determined to be 1.66 wt% by inductively coupled mass plasma spectrometry (ICP-MS) on a Thermo

Fisher iCAP Q quadrupole ICP-MS with collision cell technology.

2.2. Ex situ reactor

The stability of the as-prepared Pt₁/Fe₂O₃ SACs under various gas environments was evaluated in a fixed-bed reactor at 250 °C for 2 h. The feed gas composition was 1 vol% of the target gas and balance helium with a flow rate of 33 ml min⁻¹. For each test, ~20 mg Pt₁/Fe₂O₃ SAC was directly used without any pretreatment.

2.3. Characterization

AC high-angle annular dark-field (AC-HAADF) STEM was used to characterize the as-prepared and the gas-treated Pt₁/Fe₂O₃ SACs. Sub-ångström resolution AC-HAADF-STEM images were obtained on a JEOL JEM-ARM200F STEM/TEM, equipped with a CEOS CESCOR hexapole aberration corrector operated at 200 kV that enables an imaging resolution reaching 0.08 nm. The specimen used for the STEM investigation was prepared by dispersing the sample onto a Cu grid coated with a thin holey carbon film. X-ray photoelectron spectroscopy (XPS) characterization of the as-prepared and the gas-treated Pt₁/Fe₂O₃ SACs was conducted on a Thermo Fisher ESCALAB 250Xi x-ray photoelectron spectrometer using Al K α x-rays as the photon source.

3. Results and discussion

3.1. Fresh Pt₁/Fe₂O₃ SAC

The as-prepared sample was first characterized with sub-ångström resolution AC-HAADF-STEM and was identified as a SAC with a high number density. The HAADF-STEM imaging method adopting the STEM method, where the image intensity is approximately proportional to the square of the atomic number, has proven to be an efficient tool to characterize heterogeneous catalysts [44–46]. When combined with the AC technique, atomic resolution could be obtained, and was applied for the direct observation of metal atoms on the support surface. We have done many studies on the synthesis and AC-STEM characterization of SACs composed with different metal atoms on various supports [47, 48]. For the as-synthesized Pt₁/Fe₂O₃, as shown in figures 1(a) and (b) and many other similar low-magnification HAADF-STEM images, Pt particles or clusters were not present in the as-synthesized Pt₁/Fe₂O₃ SAC. The atomic-resolution images in figures 1(c) and (d) and the analyses of many similar images (figure S1 is available online at stacks.iop.org/NANO/29/204002/mmedia) reveal that in the as-synthesized Pt₁/Fe₂O₃ catalyst, only isolated Pt single atoms were found and that the Pt single atoms were uniformly dispersed onto the surfaces of the Fe₂O₃ nanocrystallites. We further calculated the accurate number density of Pt single atoms by equation $number\ density = ([Pt\ loading] \times N_A) / (195.08 \times [surface\ area])$, where $[Pt\ loading]$ is 1.66 wt% determined from the ICP-MS result, N_A is the Avogadro's number, and the $[surface\ area]$ is 42.55 m² g⁻¹ determined from the BET surface

area test. The accurate number density is calculated to be 1.2 atom nm⁻², which is close to the Pt single atom density (1.0 atom nm⁻²) estimated by counting on many high-resolution HAADF-STEM images, and it has reached the density limitation synthesized with an adsorption method [49]. To the best of our knowledge, it is one of the SACs with the highest number density, which is beneficial to the study of metal atom stability under various gas environments [50–52]. For the SACs with low number density, it is reported that the metal atoms do not sinter into nanoparticles or clusters and keep a single atom nature during catalytic reactions. However, it cannot be unambiguously concluded that the metals atoms are stable, because the metal atoms may be moveable on the support surfaces but cannot collide with each other and form nanoparticles or clusters during the catalytic environment because of the low number density, which needs to be further confirmed using high number density SACs.

3.2. Anchoring sites of Pt atoms

The active center of the supported metal catalyst consists of metal atoms and their vicinal atoms of the support. The configuration of the active centers is determined by the anchoring sites of the metal atoms on the oxide support, and it is critical to the charge transfer between the metal–support interaction, influencing the catalytic performances of the SACs. For SACs with low metal loading levels, many previous works have indicated that the metal atoms are anchored to the cation positions of the metal oxide supports, where the surface cation vacancies serve as anchoring sites [24, 29]. We have adopted AC-STEM images to confirm that the Pt, Ir, and Au atoms all occupied cation positions in the Pt₁/FeO_x [24, 28], Ir₁/FeO_x [27], Pt₁/ZnO [29], and Au₁/ZnO [29] SACs. Density functional theory (DFT) simulations further verify that the three-fold hollow sites on the O₃-terminated surface of Fe₂O₃(001), where the Pt atoms occupy the Fe cation positions, are the most stable anchoring sites [24, 53]. Here, we experimentally confirm it using AC-HAADF-STEM on the SAC with ultra-low metal loading. The low metal loading (0.05 wt%) Pt₁/Fe₂O₃ (denoted as 0.05Pt₁/Fe₂O₃) was comparatively synthesized using a similar adsorption method by decreasing the usage of the Pt precursor. As shown in figure 3, the density of the isolated Pt₁ atoms in the 0.05Pt₁/Fe₂O₃ is much lower than that in the Pt₁/Fe₂O₃, and the Pt atoms all occupied the positions of Fe atoms on the Fe₂O₃ surfaces, which was confirmed by checking many atomic-resolution AC-STEM images. However, the cation vacancies on the Fe₂O₃ surfaces are limited. Thus, the Pt atoms will be anchored to other site constitutions with the increase of the Pt loading level. Accordingly, the isolated Pt₁ atoms in the high metal loading SACs are not the same with different anchoring sites. Here, in our SAC with high metal loadings, Pt₁ single atoms anchored at different sites can also be directly confirmed by atomic resolution HAADF-STEM images. As shown in figure 2, when the metal loading was increased to 0.53 wt%, the anchoring sites of the Pt₁ atoms in the 0.53Pt₁/Fe₂O₃ SAC could be roughly divided into two groups: Fe-top (where the Pt₁ atoms possess the Fe position

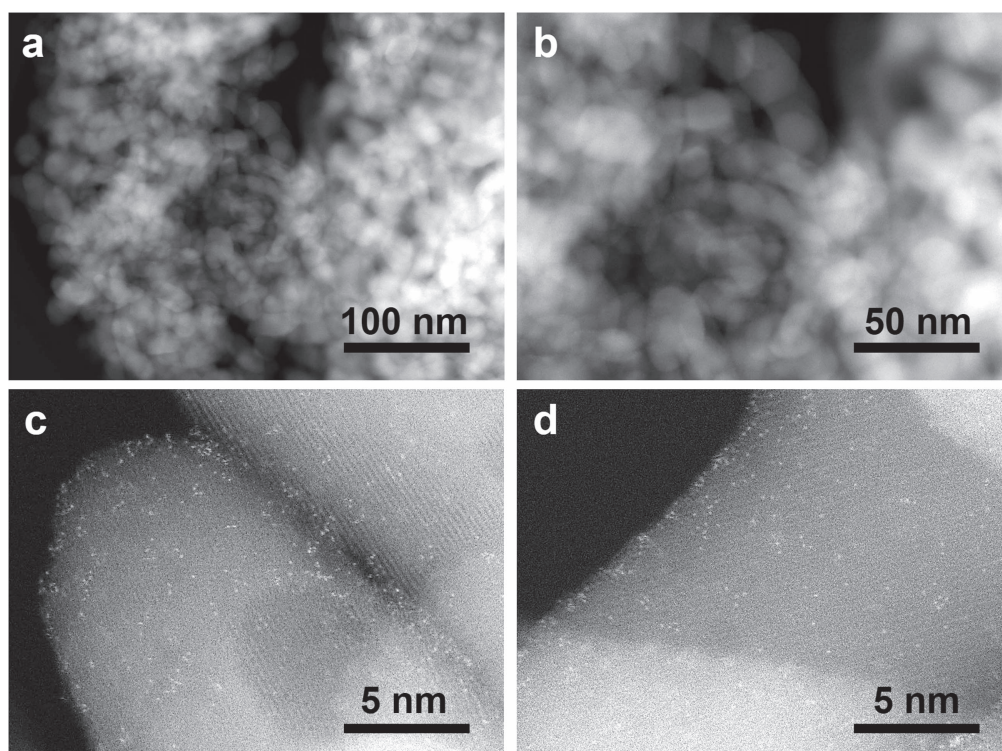


Figure 1. Low magnification (a), (b) and high resolution (c), (d) HAADF-STEM images of the as-prepared 1.66 wt% Pt₁/Fe₂O₃ SAC, revealing that it consists of only isolated Pt atoms.

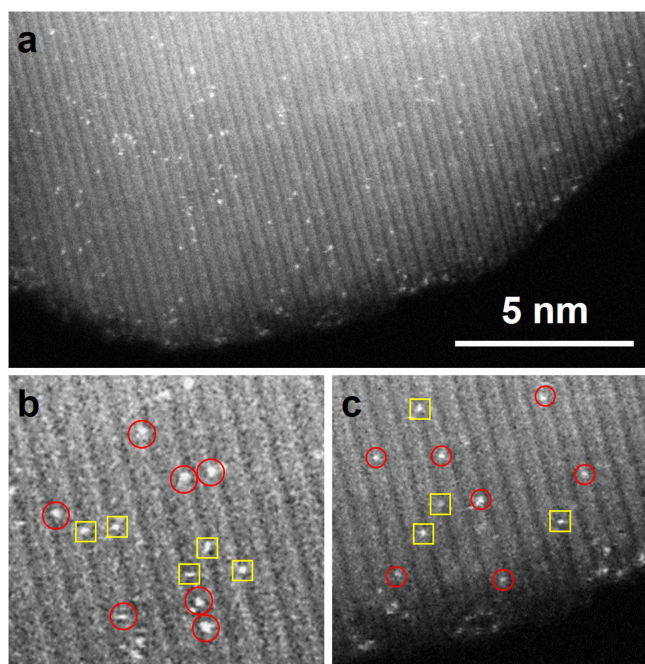


Figure 2. Typical high resolution HAADF-STEM images of sample 0.53Pt₁/Fe₂O₃. The red circles indicate the isolated Pt atoms occupied Fe-top positions, and the yellow squares indicate that the isolated Pt atoms possess O-top positions.

on the Fe₂O₃ surfaces, marked in red circles) and O-top (where the Pt₁ atoms possess the O position on the Fe₂O₃ surfaces, marked in yellow squares). It is noted that the classification method here is roughly only based on the AC-HAADF-STEM images. The refined anchoring sites may be

different for the Fe-top or O-top sites, where the Pt₁ atoms anchoring sites should be further classified into different configurations based on their interfacial environment while they show similar image in the STEM images [24, 53, 54]. Chen *et al* confirmed this using DFT computations [53]. Naoya Shibata *et al* show direct atomic-resolution images of individual Pt atoms adsorbed on TiO₂ (110) surfaces using AC STEM images with sub-ångström spatial resolution, identifying five different Pt atom adsorption sites on the TiO₂ (110) surface [54]. However, because of the irregular support surfaces and the high number density of Pt atoms in our Pt₁/Fe₂O₃ SAC, the accurate fraction of different anchoring sites cannot be directly calculated from our HAADF-STEM images.

3.3. Pt₁/Fe₂O₃ SAC under different gas environments

O₂, CO, and H₂ broadly exist in many chemical reactions such as CO oxidation, methanol steam reforming, and water-gas shift reaction. Investigation of the stability of SACs under these different gas environments provide insight into the stability of Pt atoms under reductive and oxidative environments, which is crucial to the deep understanding of catalyst activation and deactivation processes.

First, after annealing the as-prepared Pt₁/Fe₂O₃ SAC in 1 vol% O₂ at 250 °C, all the Pt single atoms remained isolated, as shown in figure 4(b). Many similar high-resolution images and low-mag HAADF-STEM images (figure S2) confirm that the Pt₁/Fe₂O₃ SAC keeps the single atom nature after annealing in O₂. The presence of O₂ molecules did not sinter the Pt single atoms at 250 °C, confirming that the

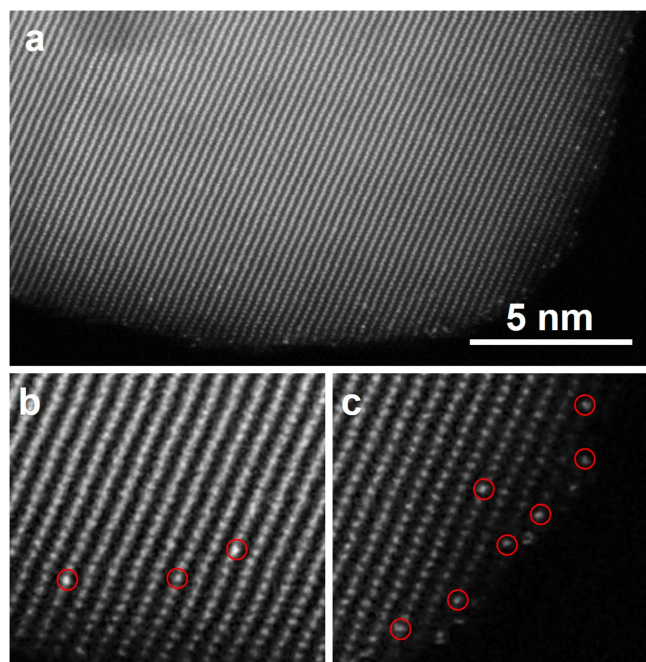


Figure 3. Typical high resolution HAADF-STEM images of sample 0.05Pt₁/Fe₂O₃. The red circles indicate the isolated Pt atoms all occupied the positions of Fe atoms at the ultra-low metal loading.

Pt₁/Fe₂O₃ SAC is stable under the oxidative environment. In our research, we also found that the Pt₁/Fe₂O₃ SAC is stable in air at room temperature even after two years. This is different from previous reports on gas-assisted sintering in air for Pt/Fe₃O₄ catalysts, where O₂ dissociates on the Pt clusters and spills over onto the support and then reacts with Fe from the bulk to create new Fe₃O₄(001) islands [40]. However, similar phenomena are not observed in our experiment. It is supposed that the calcination pretreatment is critical to the stability of Pt atoms under O₂. In our calcined Pt₁/Fe₂O₃ SAC, Pt atom is interacted with support oxygen ions after calcination, forming (Pt₁-O_n-) moieties, which is verified by the XPS result. As shown in figure 5(a), the Pt_{4f} XPS peaks of the as-prepared Pt₁/Fe₂O₃ SAC consists of two pairs of doublets: the first doublet (75.0 and 78.4 eV) and the second doublet (72.6 and 76.0 eV) correspond to Pt⁴⁺ and Pt²⁺, respectively, which reveals the presence of PtO₂ and PtO on the surface of the as-prepared Pt₁/Fe₂O₃ SAC. Peak deconvolution (figure 5(b)) revealed the contribution from Pt⁴⁺ (~64 at.%) and Pt²⁺ (~32 at.%) and the presence of metallic Pt⁰ is negligible in the fresh Pt₁/Fe₂O₃ SAC. The oxygen bonding with Pt atoms is saturated after calcination at 300 °C, thus when exposed to O₂ steam under our test condition, the O₂ molecules were not absorbed on the oxygen-saturated Pt atoms, and thus the Pt atoms will maintain the single atom nature during the exposure to O₂. This also confirms the strong metal-support interaction in our calcined Pt₁/Fe₂O₃ SAC.

Stability tests of Pt atoms under reductive atmosphere including CO (denoted as CO-Pt₁/Fe₂O₃) and H₂ (denoted as H₂-Pt₁/Fe₂O₃) were further investigated. After annealing the

as-prepared Pt₁/Fe₂O₃ SAC in 1 vol% H₂ at 250 °C for 2 h, however, the initially isolated Pt single atoms agglomerated to form small clusters (figures 6(a) and S3), clearly suggesting that the H₂ reduction treatment facilitated the sintering of the Pt single atoms. Similarly, under the CO gas treatment, the Pt single atoms moved to form subnano Pt clusters (figures 6(b) and S4). The Pt atoms are reduced to metallic Pt⁰ during the sintering process and the Pt⁴⁺ species are negligible in the reduced samples, as evidenced by the Pt_{4f} XPS spectra (figure 5). Compared to the H₂ treated sample, the size distribution of the CO treated samples is much narrower and the atomic-resolution HAADF images showed that the Pt clusters were highly disordered or amorphous-like. By counting large quantities of clusters and nanoparticles from many high resolution HAADF-STEM images, the size distributions of the gas-treated samples were obtained, as shown in figures 6(e) and (f). The size distribution of the catalyst treated with H₂ is about 1.0 ± 0.3 nm, a little bigger than that of the catalyst treated with CO (0.8 ± 0.2 nm), suggesting that the weakening effect of the (Pt₁-O_n-) bond by H₂ adsorption is stronger than that induced by CO adsorption. The gas induced metal sintering process is proposed to follow the procedure that the gas molecules firstly adsorbed onto the metal atoms, the adsorbed gas molecules then spilled over from the metal to the metal-support interaction and lastly the gas molecules at the metal-support interface extract substrate atoms at the metal-support interface thus breaking the metal-support interaction and inducing the movement of metal atoms [40, 41, 43, 50, 55–58]. In the case of CO, many reports have suggested that CO molecules strongly bond to Pt atoms, modifying the charge transfer between the metal-support interaction. And CO could be delivered to the metal-support interface and then react with lattice O atoms at the metal-support interface to create CO₂, which weakens the metal-support interaction and induces the metal movement sintering into Pt clusters [40, 59]. Under the H₂ atmosphere, adsorption and dissociation of H₂ molecules on the Pt atoms are followed by the spillover of H onto the metal-support interface to creates -OH groups [60, 61]. The surface -OH group can diffuse over the oxide surface which are known to react with O lattice atoms, leading to the desorption of water [62, 63]. This could be further verified by the O_{1s} XPS spectra of the H₂-Pt₁/Fe₂O₃ sample (figure S5), where peak deconvolution confirmed the presence of surface -OH groups (531.3 eV, ~28.7 at.%) and water species (533.1 eV, ~8 at. %). The -OH groups and water species are negligible in the as-prepared Pt₁/Fe₂O₃ and CO-Pt₁/Fe₂O₃ samples. The diffusion of the -OH groups on the Fe₂O₃ surface can accelerate the sintering of Pt atoms, thus the sintering process is faster and forms bigger Pt clusters or nanoparticles under H₂ compared to CO. However, the reduction of Fe₂O₃ with CO by extraction of lattice oxygen is much weaker than that in the case of H₂, which is confirmed by the Fe_{2p} XPS spectra in figure S6. The process of atom sintering is illustrated in figure 7.

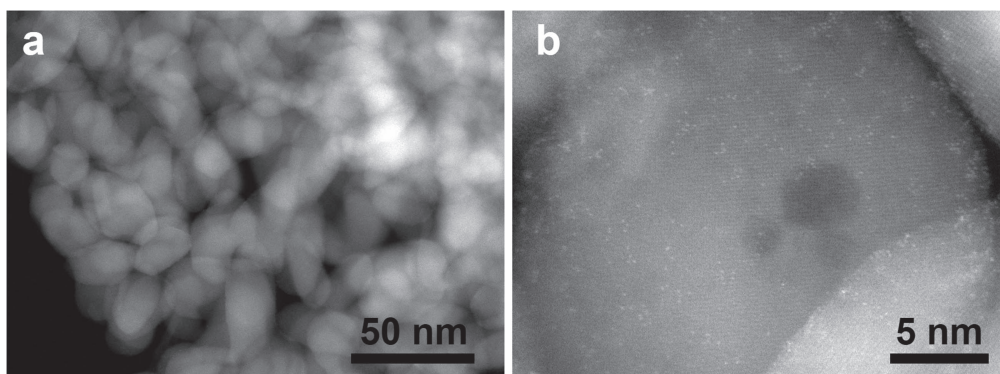


Figure 4. Low magnification and high resolution HAADF-STEM images of 1.66 wt% Pt₁/Fe₂O₃ SAC treated with O₂ at 250 °C for 2 h, revealing that O₂ does not sinter the Pt single atoms.

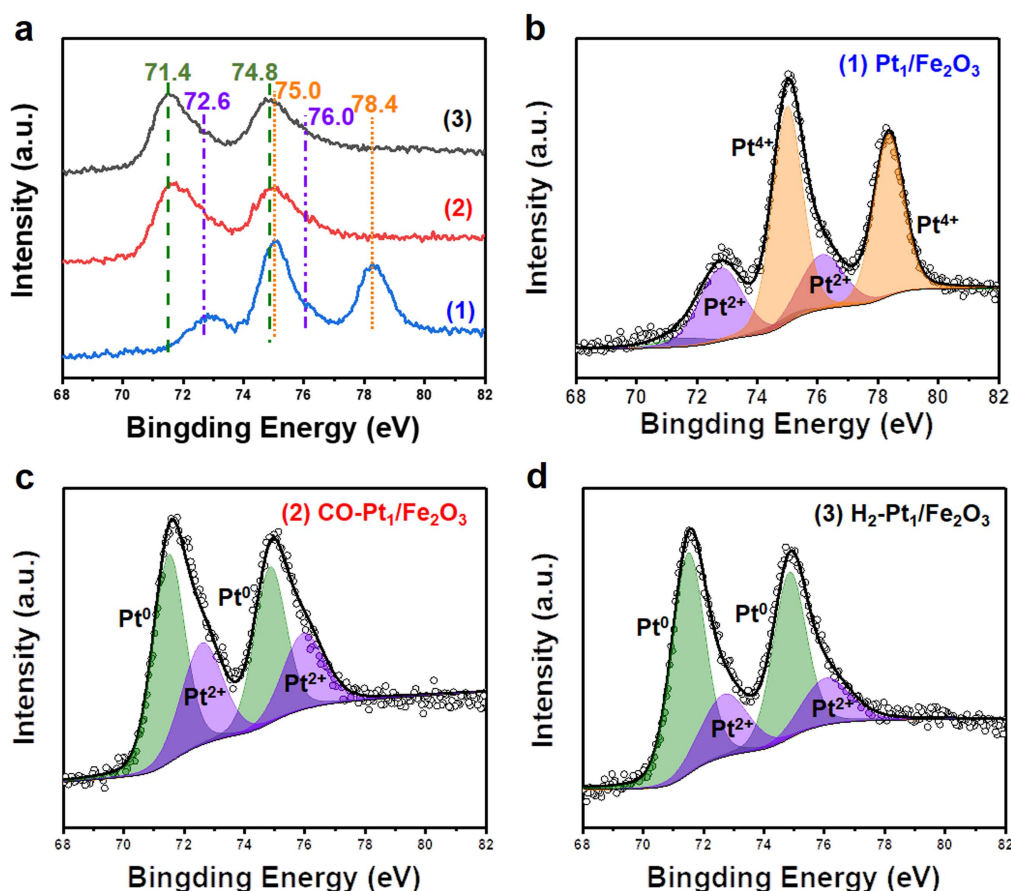


Figure 5. Pt_{4f} XPS spectra (a) and corresponding peak deconvolution (b)–(d) to reflect different contributions in the three Pt/Fe₂O₃ catalysts: (1) as-prepared Pt₁/Fe₂O₃ SAC, and after being treated with (2) CO and (3) H₂ at 250 °C for 2 h.

The effects of long-term gas treatment of supported Pt₁ SACs have also been investigated. When we extend the CO treatment at 250 °C to 24 h, the Pt clusters grew into well-crystallized Pt nanoparticles with sizes in the range of 5–10 nm, as shown in figure S7. From the high-resolution HAADF-STEM images shown in figure S7, there still exist some Pt single atoms that did not sinter into clusters, and they all occupied the Fe positions of the support surfaces. This is in accordance with previous reports that the three-fold hollow sites on the O₃-terminated surface of Fe₂O₃(001), where the

Pt atoms occupying the Fe cation positions are the most stable sites according to DFT calculations [24, 53]. This is also in line with the reported results that single atoms are stable in SACs with low metal loading where the metal atoms occupied the cation positions [24, 29, 30]. So, increasing the number of cation vacancies on the substrate surfaces should help stabilize the single metal atoms during catalytic reactions, directing the synthesis of long-term stable SACs.

When water was added into the feed gas of CO and H₂, the Pt sintering process was accelerated, and some larger Pt

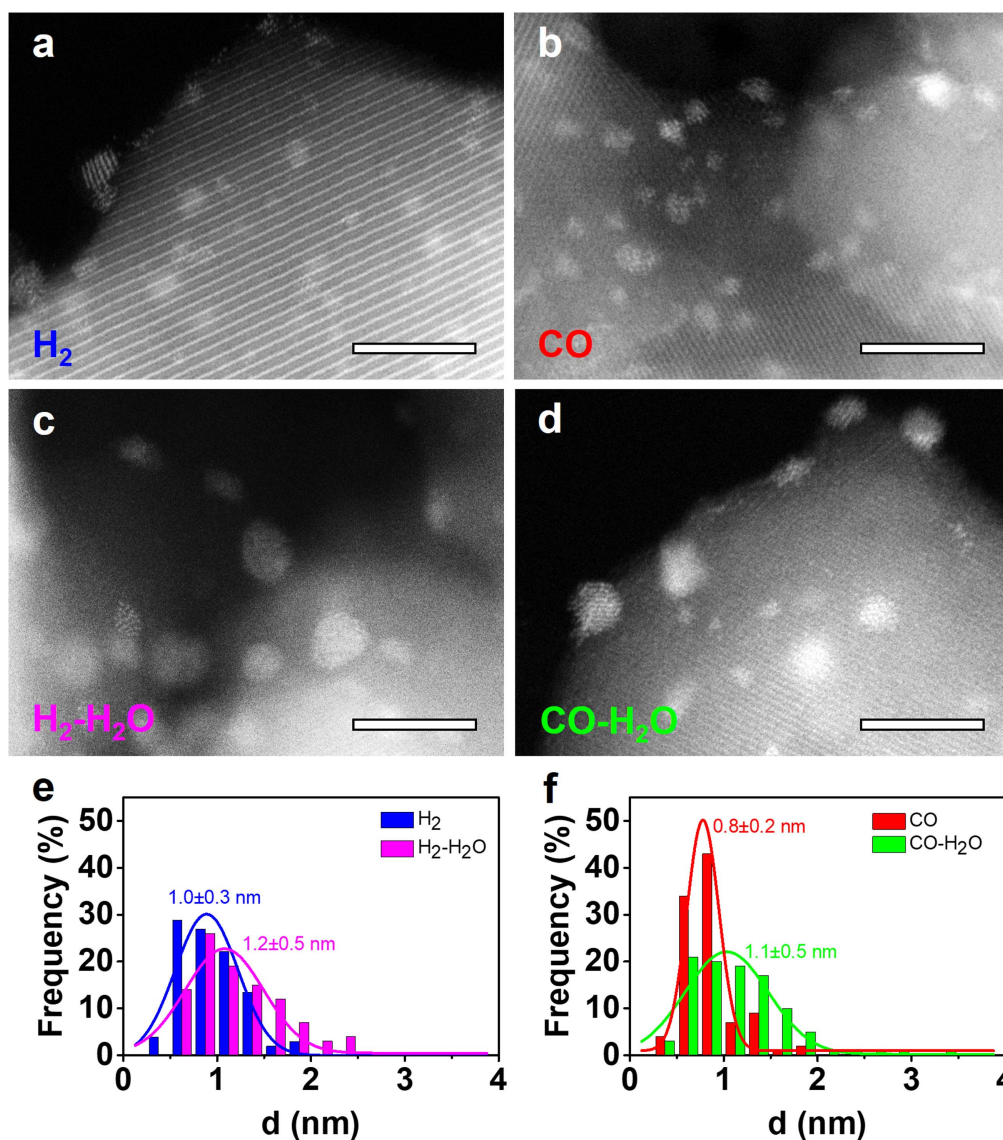


Figure 6. HAADF images of a 1.66 wt% Pt₁/Fe₂O₃ SAC after being treated with (a) H₂, (b) CO, (c) H₂-H₂O, and (d) CO-H₂O at 250 °C for 2 h; (e) and (f) the corresponding size distributions. Scale bar: 5 nm.

crystallized particles appeared (figures 5(c) and (d), S8 and S9). The size distribution of the samples treated under CO with water or H₂ with water is similar (figures 5(e) and (f)). This may result from the water species or -OH groups being associated with Pt₁ atoms forming ((OH)_{*m*}-Pt₁-O_{*n*}-) entities, that induce the charge transfer between the metal atoms and the -OH functional groups and weaken the (Pt₁-O_{*n*}) interaction, and thus facilitate the movement of the Pt atoms [28, 64–66]. Water splitting forming -OH groups at the Fe₂O₃ surface can also be achieved, which have been proven by scanning tunneling microscopy and DFT calculations [63, 67, 68]. Thus, the diffusion of the -OH groups on the Fe₂O₃ surface accelerate the sintering of Pt atoms, like that under pure H₂.

The stability tests of Pt atoms under CO or H₂ at room temperature were further investigated. After annealing the as-prepared Pt₁/Fe₂O₃ SAC in 1 vol% CO and H₂ at room

temperature for 2 h, however, the initially isolated Pt single atoms agglomerated to form small clusters under CO (figure S10), while interestingly the Pt atoms keep the single atom nature under H₂ (figure S11). Contrary to the results conducted at 250 °C, the sintering process is more efficient with CO at room temperature. This may come from the stronger adsorption of CO than that of H₂ at low temperature, which is proved by experimental result that H₂ conversion was strongly inhibited by the presence of CO in the gas phase during preferential oxidation of CO [69, 70].

From these size distributions, we concluded that at 250 °C (1) O₂ does not sinter Pt single atoms, (2) both CO and H₂ facilitate the movement of Pt atoms with a stronger effect by H₂, and (3) the presence of H₂O molecules significantly accelerates the sintering of Pt single atoms. During the sintering process, Pt single atoms anchored at different sites show different stability performances, while the O-top Pt

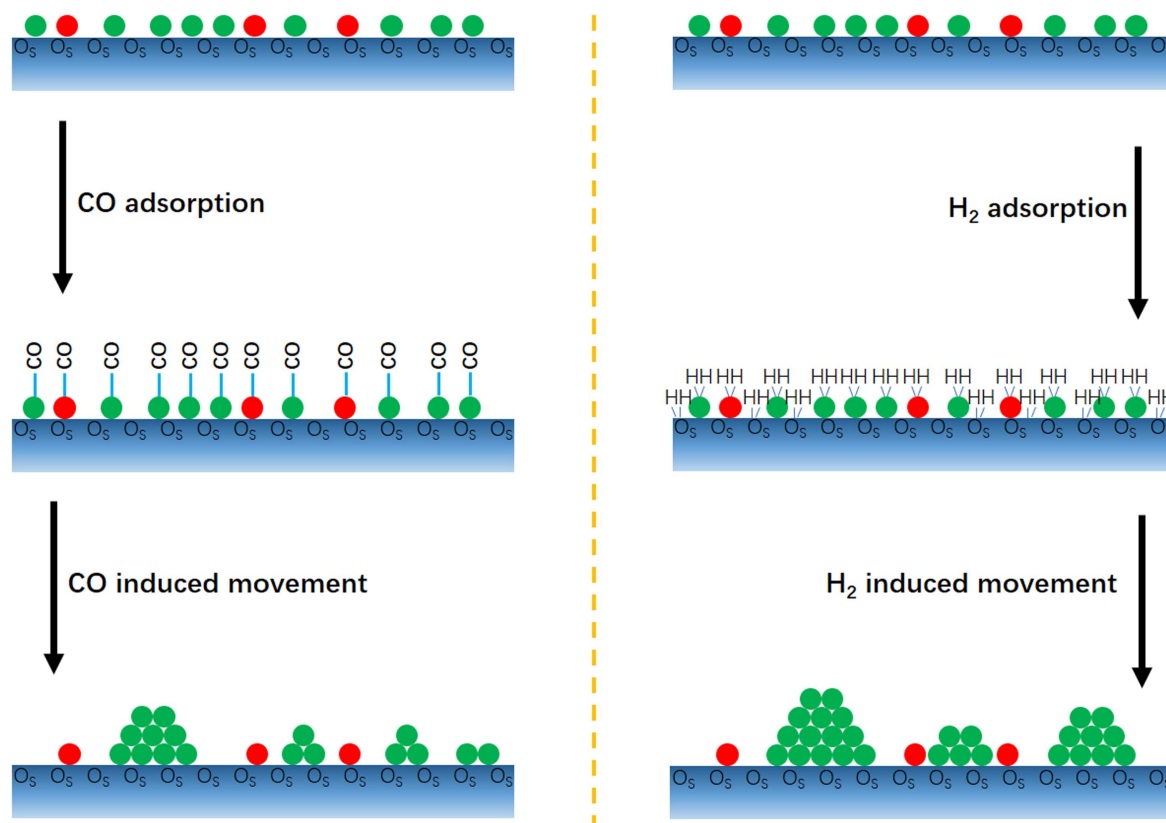


Figure 7. Scheme of the CO and H₂ induced movement of high density Pt₁/Fe₂O₃ SAC, where the different effects between CO and H₂ are highlighted. The red circles indicate the Pt atoms anchored at the Fe-top positions, which are stable during the sintering. The green circles indicate the Pt atoms anchored at the O-top positions, which are moveable during the sintering.

atoms keep the single atom nature during the treatment with a reductive environment. The extent of sintering can be well modulated by controlling the temperature, time, and gas composition, and thus could provide a protocol to obtained size controlled supported catalysts.

4. Conclusion

In summary, a Pt₁/Fe₂O₃ SAC with a high number density is synthesized using the modified adsorption method. The Pt atom density is as high as 1.2 atoms nm⁻², which reaches the number density limitation based on the adsorption mechanism. Investigation on the stability of Pt atoms under different environments suggests that the Pt atoms are stable under an oxidative atmosphere. Reductive gas including H₂ and CO weakens the metal-support interaction and induces the movement of Pt atoms, forming nanoparticles or clusters. The weakening effect of H₂ is stronger than that of CO and will be enhanced by the addition of water into the feed gas. These results will benefit the research on the stability of SACs during catalytic reactions and instruct the design of SACs with more stable anchoring sites. We also believe that with the help of AC environmental transmission electron microscopy, *in situ* characterization on the sintering process could provide us with more conclusive evidence and more detailed information in future work.

Acknowledgments

This research was supported by the National Science Foundation under CHE-1465057, the National Natural Science Foundation of China under 11674023 and 51331002, the Beijing Municipal Science and Technology Project (No. Z1711100002217074), and the Fundamental Research Funds for the Central Universities under FRF-TP-16-067A1. J L acknowledges the start-up fund of the College of Liberal Arts and Sciences of Arizona State University. We acknowledge the use of the STEM at the John M Cowley Center for High Resolution Microscopy at Arizona State University.

ORCID iDs

Sibin Duan <https://orcid.org/0000-0001-8636-9236>
Rongming Wang <https://orcid.org/0000-0003-4075-6956>

References

- [1] Munnik P, de Jongh P E and de Jong K P 2015 *Chem. Rev.* **115** 6687–718
- [2] Schlögl R 2015 *Angew. Chem., Int. Ed. Engl.* **54** 3465–520
- [3] Boudart M 1995 *Chem. Rev.* **95** 661–6
- [4] Lin J, Wang X and Zhang T 2016 *Chin. J. Catal.* **37** 1805–13

- [5] Zhai Y *et al* 2010 *Science* **329** 1633–6
- [6] Jung N, Chung D Y, Ryu J, Yoo S J and Sung Y-E 2014 *Nano Today* **9** 433–56
- [7] Ding K, Gulec A, Johnson A M, Schweitzer N M, Stucky G D, Marks L D and Stair P C 2015 *Science* **350** 189–92
- [8] Bruix A *et al* 2014 *Angew. Chem., Int. Ed. Engl.* **53** 10525–30
- [9] Yan Z, Xu Z, Yu J and Jaroniec M 2015 *Environ. Sci. Technol.* **49** 6637–44
- [10] Crampton A S, Rotzer M D, Ridge C J, Schweinberger F F, Heiz U, Yoon B and Landman U 2016 *Nat. Commun.* **7** 10389
- [11] Tauster S J, Fung S C, Baker R T and Horsley J A 1981 *Science* **211** 1121–5
- [12] An K, Alayoglu S, Musselwhite N, Plamthottam S, Melaet G, Lindeman A E and Somorjai G A 2013 *J. Am. Chem. Soc.* **135** 16689–96
- [13] Zhou Y, Li Y and Shen W 2016 *Chem. Asian J.* **11** 1470–88
- [14] Li Y and Shen W 2014 *Chem. Soc. Rev.* **43** 1543–74
- [15] Yoon B, Hakkinen H, Landman U, Worz A S, Antonietti J M, Abbet S, Judai K and Heiz U 2005 *Science* **307** 403–7
- [16] Campbell C T 2012 *Nat. Chem.* **4** 597–8
- [17] Najafshirtari S, Guardia P, Scarpellini A, Prato M, Marras S, Manna L and Colombo M 2016 *J. Catal.* **338** 115–23
- [18] Kondratenko V A, Berger-Karin C and Kondratenko E V 2014 *ACS Catal.* **4** 3136–44
- [19] An N, Li S, Duchesne P N, Wu P, Zhang W, Lee J-F, Cheng S, Zhang P, Jia M and Zhang W 2013 *J. Phys. Chem. C* **117** 21254–62
- [20] Zhu J, Yang M L, Yu Y D, Zhu Y A, Sui Z J, Zhou X G, Holmen A and Chen D 2015 *ACS Catal.* **5** 6310–9
- [21] Nie L *et al* 2017 *Science* **358** 1419–23
- [22] Zhang S, Li J, Xia Z, Wu C, Zhang Z, Ma Y and Qu Y 2017 *Nanoscale* **9** 3140–9
- [23] Fu Q, Saltsburg H and Flytzani-Stephanopoulos M 2003 *Science* **301** 935–8
- [24] Qiao B, Wang A, Yang X, Allard L F, Jiang Z, Cui Y, Liu J, Li J and Zhang T 2011 *Nat. Chem.* **3** 634–41
- [25] Novotny Z, Argentero G, Wang Z, Schmid M, Diebold U and Parkinson G S 2012 *Phys. Rev. Lett.* **108** 216103
- [26] Wang Y G, Mei D, Glezakou V A, Li J and Rousseau R 2015 *Nat. Commun.* **6** 6511
- [27] Lin J, Wang A, Qiao B, Liu X, Yang X, Wang X, Liang J, Li J, Liu J and Zhang T 2013 *J. Am. Chem. Soc.* **135** 15314–7
- [28] Lou Y and Liu J 2017 *Ind. Eng. Chem. Res.* **56** 6916–25
- [29] Gu X, Qiao B, Huang C, Ding W, Sun K, Zhan E, Zhang T, Liu J and Li W-X 2014 *ACS Catal.* **4** 3886–90
- [30] Qiao B, Liang J, Wang A, Xu C, Li J, Zhang T and Liu J 2015 *Nano Res.* **8** 2913–24
- [31] Peng S Y, Xu Z N, Chen Q S, Wang Z Q, Lv D M, Sun J, Chen Y M and Guo G C 2015 *ACS Catal.* **5** 4410–7
- [32] Ramos E, Davin L, Angurell I, Ledesma C and Llorca J 2015 *ChemCatChem* **7** 2179–87
- [33] Varga E, Pusztai P, Oszko A, Baan K, Erdohelyi A, Konya Z and Kiss J 2016 *Langmuir* **32** 2761–70
- [34] Hellström M, Spångberg D, Hermansson K and Broqvist P 2014 *J. Phys. Chem. C* **118** 6480–90
- [35] Farmer J A and Campbell C T 2010 *Science* **329** 933–6
- [36] Kwak J H, Hu J, Mei D, Yi C W, Kim D H, Peden C H, Allard L F and Szanyi J 2009 *Science* **325** 1670–3
- [37] Kim Y T, Ohshima K, Higashimine K, Uruga T, Takata M, Suematsu H and Mitani T 2006 *Angew. Chem., Int. Ed. Engl.* **45** 407–11
- [38] Zhang S, Katz M B, Dai S, Zhang K, Du X, Graham G W and Pan X 2017 *J. Phys. Chem. C* **121** 17348–53
- [39] Xiong H, Lin S, Goetze J, Pletcher P, Guo H, Kovarik L, Artyushkova K, Weckhuysen B M and Datye A K 2017 *Angew. Chem., Int. Ed. Engl.* **56** 8986–91
- [40] Bliem R, van der Hoeven J, Zavodny A, Gamba O, Pavelec J, de Jongh P E, Schmid M, Diebold U and Parkinson G S 2015 *Angew. Chem., Int. Ed. Engl.* **54** 13999–4002
- [41] Bliem R, van der Hoeven J E, Hulva J, Pavelec J, Gamba O, de Jongh P E, Schmid M, Blaha P, Diebold U and Parkinson G S 2016 *Proc. Natl Acad. Sci. USA* **113** 8921–6
- [42] Parkinson G S, Novotny Z, Argentero G, Schmid M, Pavelec J, Kosak R, Blaha P and Diebold U 2013 *Nat. Mater.* **12** 724–8
- [43] Moses-DeBusk M, Allard L F, Blom D A and Narula C K 2015 *ChemCatChem* **7** 2391–6
- [44] Liu J 2005 *J. Electron Microsc.* **54** 251–78
- [45] Liu J Y 2011 *ChemCatChem* **3** 934–48
- [46] Liu J 2017 *Chin. J. Catal.* **38** 1460–72
- [47] Allard L F, Duan S and Liu J 2016 *Microsc. Microanal.* **22** 876–7
- [48] Duan S B, Wang R M and Liu J Y 2015 *Microsc. Microanal.* **21** 1729–30
- [49] Brown G E *et al* 1999 *Chem. Rev.* **99** 77–174
- [50] Jones J *et al* 2016 *Science* **353** 150–4
- [51] Choi C H, Kim M, Kwon H C, Cho S J, Yun S, Kim H T, Mayrhofer K J, Kim H and Choi M 2016 *Nat. Commun.* **7** 10922
- [52] Yang M, Allard L F and Flytzani-Stephanopoulos M 2013 *J. Am. Chem. Soc.* **135** 3768–71
- [53] Li F, Li Y, Zeng X C and Chen Z 2015 *ACS Catal.* **5** 544–52
- [54] Chang T Y, Tanaka Y, Ishikawa R, Toyoura K, Matsunaga K, Ikuhara Y and Shibata N 2014 *Nano Lett.* **14** 134–8
- [55] Kaminski P and Ziolek M 2016 *Appl. Catal. B* **187** 328–41
- [56] Bradley S A, Sinkler W, Blom D A, Bigelow W, Voyles P M and Allard L F 2011 *Catal. Lett.* **142** 176–82
- [57] Kim J, Noh M C, Doh W H and Park J Y 2016 *J. Am. Chem. Soc.* **138** 1110–3
- [58] Moliner M, Gabay J E, Kliever C E, Carr R T, Guzman J, Casty G L, Serna P and Corma A 2016 *J. Am. Chem. Soc.* **138** 15743–50
- [59] Widmann D and Behm R J 2014 *Acc. Chem. Res.* **47** 740–9
- [60] Benvenutti E V, Franken L, Moro C C and Davanzo C U 1999 *Langmuir* **15** 8140–6
- [61] Fröhlich G and Sachtler W M H 1998 *J. Chem. Soc. Faraday Trans.* **94** 1339–46
- [62] Huang W and Ranke W 2006 *Surf. Sci.* **600** 793–802
- [63] Parkinson G S, Novotný Z, Jacobson P, Schmid M and Diebold U 2011 *J. Am. Chem. Soc.* **133** 12650–5
- [64] Zhang S, Li X-S, Chen B, Zhu X, Shi C and Zhu A-M 2014 *ACS Catal.* **4** 3481–9
- [65] Li G, Li L, Yuan Y, Shi J, Yuan Y, Li Y, Zhao W and Shi J 2014 *Appl. Catal. B* **158–159** 341–7
- [66] Saavedra J, Doan H A, Pursell C J, Grabow L C and Chandler B D 2014 *Science* **345** 1599–602
- [67] Yamamoto S *et al* 2010 *J. Phys. Chem. C* **114** 2256–66
- [68] Wendt S, Matthiesen J, Schaub R, Vestergaard E K, Laegsgaard E, Besenbacher F and Hammer B 2006 *Phys. Rev. Lett.* **96** 066107
- [69] Liu K, Wang A and Zhang T 2012 *ACS Catal.* **2** 1165–78
- [70] Qiao B, Wang A, Li L, Lin Q, Wei H, Liu J and Zhang T 2014 *ACS Catal.* **4** 2113–7